HHS Public Access

Author manuscript

Bioconjug Chem. Author manuscript; available in PMC 2019 May 06.

Published in final edited form as:

Bioconjug Chem. 2017 May 17; 28(5): 1481–1490. doi:10.1021/acs.bioconjchem.7b00153.

Targeting and Internalization of Liposomes by Bladder Tumor Cells Using a Fibronectin Attachment Protein-derived Peptide-Lipopolymer Conjugate

Young Lee, **Erin Kischuk**, **Scott Crist**, **Timothy L. Ratliff**, and **David H. Thompson***

Purdue University Center for Cancer Research, Multi-disciplinary Cancer Research Facility, Purdue University, 1201 W. State Street, West Lafayette, IN 47907

Abstract

A synthetic peptidolipopolymer conjugate, incorporated into liposomes to promote specific binding to the fibronectin (FBN) matrix surrounding bladder tumor cells and promote cellular internalization of FBN-integrin complexes, is reported. The peptide promotes association with MB49 mouse model bladder tumor cells in a sequence-specific and concentration-dependent manner, with the maximum cell association occurring at 2 mol% RWFV-PEG2000-DSPE. Double PEGylation of the liposome membrane (i.e., 4 mol% mPEG1000-DSPE + 2 mol% RWFV-PEG2000-DSPE) enhanced binding by > 1.6-fold, by improving ligand presentation on the liposome surface. The sequence specificity of the peptide-lipopolymer construct was confirmed by comparing liposomes containing RWFV-PEG2000-DSPE with scrambled and non-peptidic lipopolymer liposomal formulations. MB49 tumor-bearing mice showed greater mean radiance values for FAP peptide-targeted liposomes in tumor-associated regions of interest than for non-targeted and scrambled peptide liposome formulations. These findings suggest that peptide-modified liposomes may be an attractive vehicle for targeted delivery to bladder tumors *in vivo*.

Introduction

Bladder carcinoma is the most common malignancy of the urinary tract.[1] It is the fourth most common cancer in men and eleventh most common in women, translating to a frequency of 1 in 26 for men and 1 in 88 for women.[1–4,5] Although 70–80% of bladder cancer cases are categorized as superficial disease (nonmuscle invasive bladder cancer; NMIBC) that is surgically treatable with a high survival rate (88–98%), surgical resection is also associated with a high recurrence rate (70%) that requires extensive follow-up.[3–4, 7] It is believed that the high recurrence rate may be a consequence of poor detection technology.[6] This approach creates challenges for discriminating tumor areas from normal bladder tissue and for detecting small lesions, potentially leading to lost treatment opportunities.

Mycobacterium bovis bacillus Calmette-Guerin (BCG) is the primary agent used for adjuvant intravesical immunotherapy of early stage bladder cancer. The therapy consists of catheter-mediated instillation of live BCG bacteria into the bladder lumen to promote

* Corresponding author davethom@purdue.edu.

Supporting Information Available

adsorption of the organism to exposed fibronectin near exposed bladder tumor cells that lack a well-formed glycosaminoglycan (GAG) layer in the urothelium. BCG adsorption causes inflammation and induces an inflammatory response to clear both the adherent BCG and the neighboring bladder cancer cells.[8–9] Although BCG immunotherapy has been used successfully for over 30 years, the utility of this treatment can be limited by high local morbidity, risk of systemic mycobacterial infection, and limited patient tolerance due to severe pain and irritation.

Intravesical administration has also been used for local delivery of high doses of chemotherapeutic agent such as mitomycin C within the bladder to reduce the risk of severe systemic toxicity.[10–11] Unfortunately, constant urine influx and periodic voiding limits the effectiveness of chemotherapeutic approaches since the agent can typically only be retained in the bladder for ≤2 hours.

Despite the long clinical experience with BCG, its detailed mechanism of action is incompletely understood. Nonetheless, it is known that retention of BCG within the bladder and internalization of the bacterium by urothelial cells is required to trigger an antitumor response.[9,12] The unique organization of the bladder lining is composed of an impermeable translational epithelium[13] and GAG layer that is the principal barrier to permeability of small molecules, preventing them from reaching the underlying tight junctions and cell membranes. However, since bladder cancer cells are less differentiated, they are less polarized and exhibit diminished expression of GAG and uroplakins,[14] leading to tumor cell exposure to the bladder lumen and increased accessibility of small molecules and BCG to the tumor site. Unfortunately, small molecule therapeutics are washed out during periodic voiding, whereas BCG undergoes an increased contact time by retention at the tumor site(s).

Previous reports have shown that BCG is retained within the bladder by attachment to the fibronectin (FBN) matrix in the tumor microenvironment in a protein sequence-specific manner.[12, 15–17] The protein responsible for this adhesion is a virulence factor for several extracellular pathogenic bacteria, leading to their enhanced colonization of mucosal surfaces.[15] The high affinity BCG-FBN interaction is mediated by a bacterial adhesin known as fibronectin attachment protein (FAP). FAP is a member of the family of FBN-binding glycoproteins that are highly conserved and expressed by several species of mycobacteria.[18] FAP has been identified as the key element that mediates BCG attachment and internalization by bladder tumor cells. This is achieved by FAP binding to $\alpha_5\beta_1$ integrin-FBN complexes present on exposed tumor cells in the lumen of the bladder.[14, 19–20] Turnover of fibronectin through receptor-mediated endocytosis of β_1 integrin-FBN complexes occurs via Cav-1.[21] This host cell response likely plays an important role in the immunotherapeutic activity of BCG.

Nanoparticle-based drug delivery has been widely studied as a potential means to overcome the lack of tissue specificity of conventional cancer chemotherapy.[22–23] Liposomes are one class of lipid-based nanoparticles derived from naturally occurring phospholipids that feature high biocompatibility, biodegradability, and low immunogenicity properties. Liposomes have been widely used to improve the therapeutic index of low molecular weight drugs by modifying the solubility and biodistribution of the agent, while also prolonging its

biological half-life and reducing its systemic toxicity.[24–25] Liposomes can be prepared in a size controlled manner (50–150 nm)[26–27] and can be surface functionalized to confer long-circulation or target-specific adhesion properties. Grafting of poly(ethylene glycol) (PEG) polymers onto the liposome surface is a common technique that reduces the particle aggregation and protects the liposome from rapid degradation by the host immune system, [28–29] whereas incorporation of ligands on the liposome surface enables the delivery of drugs to specific target tissue areas.

Liposome PEGylation has been previously employed to prevent aggregation and enhance particle stability in the bladder lumen.[30–31] Unfortunately, this strategy does not overcome the low retention and frequent voiding challenges inherent in bladder tumor therapy. Targeted formulations have been developed to address this issue, with bladder cancer specific PLZ4 ligands developed for micelle formulations[32] and transferrin conjugated liposomes[33] reported for the selective delivery of paclitaxel and the photodynamic sensitizer, $AlPcS_4^{4-}$, respectively. Moreover, bioadhesive nanoparticles comprised of chitosan/poloxamer gels were developed to increase the residence time in the bladder[34]. However, it was demonstrated that some PLZ4-micelles ended up in the liver and lungs, whereas transferrin-liposomes competed with transferrin in blood, and poloxamer gels lost their stability at body temperature, thus requiring additional steps to overcome these limitations that impact their practical application in the clinic.

In a previous study, we reported that full length hexahistidine-FAP could trigger the selective binding and uptake of nitrilotriacetic acid-modified liposomes by MB49 mouse bladder cancer cells.[14] This work also showed that multivalent FAP-bearing liposomes induced the crosslinking of FBN-integrin complexes, leading to microaggregation-induced internalization via the caveolar pathway when the liposome size (< 70 nm) and FAP ligand surface density were controlled. Unfortunately, full length FAP is prone to aggregation, making this liposome formulation a challenging one to deploy from a routine therapeutic perspective due to the need for protein expression and purification immediately prior to use. In an effort to obviate this problem, while retaining the favorable properties of FAP, we sought the development of a targeted liposomal delivery system using a synthetic peptide construct derived from FAP to promote selective and efficient localization of the carrier system at the tumor site.

Ratliff and coworkers characterized the FAP protein sequence and identified the residues responsible for FBN binding via alanine scanning.[15] The key sequence involved in FBN binding was identified as residues 269–292 (i.e., GNRQRWFVVWLGSTNDPVDKVAAK). This sequence contains several charged and polar residues outside the proline rich areas of the protein. A minimal binding sequence at residues 269–280 (i.e., GNRQRWFVVWLG) was further identified as the domain that was most responsible for functional activity, with the RWFV sequence being essential for FBN binding.[16]

We sought to leverage this information to develop a liposomal carrier system that displayed the unique binding specificity and affinity characteristics of FAP, while improving the stability and batch-to-batch uniformity and manufacturability of a targeted liposome formulation. Our efforts focused on the preparation of a synthetic FAP peptide,

GNRQRWFVVWLGSTNDPV,[15] for ligation to the distal terminus of a PEG2000-DSPE lipopolymer for incorporation within a liposome formulation to promote the site specific binding and internalization of this carrier system by MB49 cells (Figure 1). In brief, we find that this system can successfully target bladder tumors *in vitro* and *in vivo*, thus suggesting that it may form the basis of an important new bladder cancer therapeutic vehicle.

Results and Discussion

Synthesis of FAP peptide-lipopolymer conjugates

We sought the preparation of an octadecameric FAP peptide-lipopolymer construct that could recapitulate the high affinity binding of FAP with fibronectin, while avoiding some of the aggregation and instability issues associated with the full length protein. The FAP-derived peptide, GNRQ**RWFV**VWLGSTNDPV-propargylglycine, containing the essential RWFV tetrapeptide sequence for FBN engagement and a terminal alkynylglycine residue for subsequent CuAAC conjugation, was prepared by SPPS. The alkynyl moiety was installed at the C-terminus of FAP peptide to enable proper orientation of the FBN binding sequence after CuAAC-mediated coupling with the lipopolymer for liposome incorporation. The hydrophobic character of the peptide and lipopolymer components required a solvent mixture (8:2 DMF/H_2O) and bath sonication to sufficiently solubilize the peptide and lipid components for an efficient coupling reaction. After RP-HPLC purification of the coupling product between the peptide with N_3-PEG2000-DSPE, MALDI-TOF mass spectrometry analysis revealed a predominant signal that was consistent with the molecular weight of the GNRQRWFVVWLGSTNDPV-PEG2000-DSPE FAP peptide-lipopolymer conjugate at m/z ~ 5200 (Figure 2). The FBN targeted construct, RWFV-PEG2000-DSPE, and the corresponding scrambled peptide construct, WVRF-PEG2000-DSPE, were used in subsequent liposome experiments to evaluate the role of target ligand density and sequence specificity on bladder tumor cell targeting efficiency.

Preparation and characterization of FAP peptide-targeted liposomes

The FAP peptide conjugates were formulated with DPPC and cholesterol to produce dispersions that could remain stable during storage and under *in vitro* and *in vivo* conditions.[35] Probe sonication was used to fabricate SUV particles capable cellular internalization via the clathrin-independent, caveolae-dependent uptake pathway having a strict < 70 nm diameter size restriction.[14] The formulations were also designed to present multiple copies of targeting peptide ligand on the liposome surface to promote MB49 cell association and internalization. Dynamic light scattering analysis of multivalent FAP peptide-targeted liposomes (Figure SI 1a) revealed a mean hydrodynamic radius of 58 ± 22 nm (PDI 0.177) and a mean ζ potential of −36 ± 7.5 mV that has been reported to limit non-specific liposome uptake.[36] Negative stain TEM analysis (Figure SI 1b) reveals the presence of a spherical, unilamellar liposome population. In this formulation, the FAP peptide ligand is immobilized on the liposome surface through hydrophobic interactions between the DSPE lipid anchor and the membrane bilayer[37] and connected via a flexible hydrophilic polymer tether to provide conformational flexibility for optimizing the engagement of the ligand with its FBN binding partner.[38]

Cell association induced by targeting mechanism

The targeting efficiency of FAP peptide-targeted liposomes for FBN:integrin complexes was evaluated in murine urothelial carcinoma MB49 cells by monitoring their liposome-associated fluorescence intensities via flow cytometry. Previous studies have shown that multivalent liposomes need an optimal surface ligand density with appropriate ligand separation to promote receptor crosslinking and internalization.[14, 39] We tested this concept by varying the FAP peptide-lipopolymer concentration (0.1, 0.5, 1, 2, 4 mol%) in the liposomal membrane and measuring its impact on the magnitude of MB49 cell association. Cell binding progressively increased with increased FAP peptide-lipopolymer concentration in the liposome up to a maximum at 2 mol%; however, the extent of cell association decreased with further increases in RWFV-PEG2000-DSPE loadings to 4 mol% (Figure 3A). We attribute these findings to a target ligand oversaturation phenomenon wherein the peptide targeting ligands are entangled and/or buried within the PEG corona and unavailable to engage the FBN:integrin complexes.[40] In addition, it is also known that increasing the average number of ligands per nanoparticle increases the chance that two ligands exist in close proximity, resulting in a competition between multivalently bound nanoparticles and unbound nanoparticles for the receptors available on the cell surface.[39] Regardless of the mechanism operating in this system, we elected to use liposomes bearing 2 mol% of FAP peptide-lipopolymer in all subsequent studies.

We then compared the extent of MB49 cell association with FAP peptide-free and FAP peptide-containing liposome formulations. The data in Figure 3B show that liposomes containing 2 mol% RWFV-PEG2000-DSPE had significantly greater cell association than the non-targeted (2 mol% mPEG2000-DSPE) or control (no liposomes) groups. The minimal cell association displayed by the non-targeted liposomes suggest that the PEG corona surrounding the liposome serves as an effective barrier toward blocking non-specific adsorption to MB49 cells.

Intracellular trafficking of FAP-peptide targeted liposomes

Since cell-carrier system interactions can greatly impact their internalization rate and therapeutic efficacy,[41] we monitored the binding and intracellular trafficking of FAP peptide-lipopolymer targeted liposomes by confocal microscopy. Using FITC-labeled liposomes, we observed that targeted liposomes had an enhanced binding to MB49 cells relative to non-targeted liposomes when monitored under the same imaging parameters (Figure 4A), a finding that is consistent with the flow cytometry observations in Figure 3B. Time-dependent z-stack images of targeted liposomes (2 mol% RWFV-PEG2000-DSPE) showed that 2 h after liposome addition, most of the particles were plasma membrane bound, with some internalization and co-localization with the acidic lysosomes as indicated by yellow fluorescence in the images due to overlap of the red AlexaFluor® 680 WGA-stained lysosome and green FITC-labeled liposomes (Figure 4B). After 10 h incubation, more internalization and co-localization of the targeted liposomes with the lysosomal compartments was apparent. These findings suggest that binding and internalization of FAP peptide-lipopolymer targeted liposomes occurs in MB49 cells in a kinetic window that is similar to that reported for full length FAP internalization via the caveolar pathway[14]

Assessment of peptide sequence specificity toward targeting of FBN:integrin complexes

To further probe the effectiveness and sequence specificity of FAP peptide targeting for the FBN:integrin complexes in MB49 cells, we synthesized a FAP peptide-lipopolymer containing WVRF, a scrambled version of the key RWFV binding motif in the targeting peptide sequence, to evaluate its impact on fibronectin binding activity. Scrambled peptides are often used as negative controls to show that a specific sequence is critical for function.[42] Comparison of the time-dependent MB49 cell association of targeted (RWFV) and scrambled (WVRF) FAP peptide-modified liposomes showed that liposome-based Cy5.5 fluorescence increased with time for 2 mol% RWFV-PEG2000-DSPE containing liposomes, whereas the Cy5.5 fluorescence of MB49 cells remained constant with time for the 2 mol% WVRF-PEG2000-DSPE (scrambled) liposomes and control groups (Figure 5). Weak binding due to the scrambled tetrapeptide sequence was expected since the flanking sequences in the adhesion protein are thought to contribute to binding affinity via charged amino acid interactions. Nonetheless, these findings underscore the importance of the RWFV tetrapeptide sequence for specific binding to FBN:integrin complexes in MB49 cells.

Cytotoxicity assay

The tolerance of MB49 cells toward liposomes containing FAP peptide-lipopolymers was studied using LIVE/DEAD® analysis. This assay is based on the irreversible reaction of viability dyes with the primary amine groups of cellular proteins in live versus dead cells[43] that can easily be discriminated by flow cytometry. We found that all constructs were not toxic, regardless of the presence or type of FAP peptide-lipopolymer present in the liposome formulation (Figure SI 2). The non-toxic targeted delivery system maximizes the chance to treat the target cells efficiently without risking healthy cells or inducing side effects.

Improvement in Cell Association Efficiency by Double PEGylation

As the data in Figure 3A shows, the FAP peptide targeting moieties can be encumbered by entanglement in the PEG corona of the liposome. We reasoned that double PEGylation with two different PEG chain lengths might improve the targeting efficiency by reducing the masking effect of peptide that is embedded within long PEG chains. Thus, a higher concentration of short mPEG1000 polymer was used as a non-specific blocking layer while a lower concentration of longer PEG2000 bearing the peptide targeting group was used to limit interactions with the shorter PEG corona. This architecture was selected to produce a dense mushroom layer of mPEG1000 that would promote stretching of the PEG2000 chains to more efficiently present the peptide targeting ligand to the FBN:integrin complexes on the cell surface. Liposome formulations containing only short PEG polymers (4 mol% mPEG1000-DSPE) and blends with different FAP peptide-lipopolymer constructs (non-targeted, 2 mol% mPEG2000-DSPE), scrambled (2 mol% WVRF-PEG2000-DSPE), and targeted (2 mol% RWFV-PEG2000-DSPE) were prepared. Characterization data indicated that the size and ζ potential were similar in these preparations (data not shown). Double PEGylation led to a significant boost in targeting efficiency for the targeted liposome formulation relative to the scrambled and non-targeted liposome groups (Figure 6). These findings are in agreement with the hypothesis that the targeting ligands are more available for target engagement due to reduced encumbrance from occupancy within the PEG corona.

Based on these findings, liposomal formulations employing double PEGylation with 2% of FAP peptide-lipopolymer targeting was used in all subsequent studies.

Mouse Bladder Tumor Model *In Vivo* Analysis

The tumor homing activity of *in vitro* optimized FAP peptide-lipopolymer targeted liposomes was then evaluated in an orthotopic model of bladder cancer to investigate the *in vivo* targeting efficiency of these vehicles. MB49-Luc cells were instilled via catheter into the bladder of female Balb/c mice. Mice with developed tumors at Day 9 – 11 were selected based on their bioluminescent signal intensity after i.p. injection of luciferin using an *in vivo* imaging system (Spectral Ami Optical Imaging System). Tumor-bearing mice were then treated intravesically with non-targeted (2 mol% mPEG2000-DSPE), scrambled (2 mol% WVRF-PEG2000-DSPE), or targeted (2 mol% RWFV-PEG2000-DSPE) liposome suspensions containing 4 mol% mPEG1000-DSPE and 0.5 mol% Cy5.5-DSPE and imaged after 1 h for both luminescent and fluorescent signals. The data in Figure 7A show the color-coded luminescent signal intensities from bladder tissue of luciferin treated animals. Tumor positive areas appear in most animals and are heterogeneous in size. Figure 7B depicts the Cy5.5 fluorescence intensities in the same tissues due to liposome-mediated binding to the bladder tissue. Then whole bladder was assigned as a region of interest (ROI) to evaluate the overall binding events. This data shows that RWFV-PEG2000-DSPE targeted liposomes bind bladder tumors more efficiently than the WVRF-PEG2000-DSPE scrambled or non-targeted liposomes ($p \leq 0.05$ in all cases; Figure 7C). Conversely, scrambled liposomes displayed reduced tumor engagement than targeted liposomes. Non-targeted liposomes had little or no binding compared to non-treated controls, confirming that non-specific binding is minimal in the absence of synthetic FAP peptide-lipopolymer. These findings suggest that synthetic FAP peptide-lipopolymers contribute to enhanced binding of liposomes to bladder tumors *in vivo* in a sequence-specific manner.

Conclusions

This work demonstrates that FAP peptide-lipopolymers are capable of binding to MB49 cells in a concentration- and time-dependent manner. Optimal cell association occurred using liposomes bearing 2 mol% RWFV-PEG2000-DSPE combined with 4 mol% mPEG1000-DSPE in a double PEGylation strategy that presumably enhances FAP peptide presentation to FBN:integrin complexes in the bladder tumor target cells. These formulations were non-toxic and could be reproducibly prepared with diameters below 70 nm, a required feature to enable uptake via the caveolar pathway. Orthotopic bladder tumor model experiments also showed that sequence-specific targeting of liposomes could be successfully translated to the *in vivo* setting. These findings suggest that FAP peptide-targeted liposomes may serve as an improved therapeutic vehicle for bladder cancer treatment by utilizing the binding specificity of FAP peptide for the tumor microenvironment, while offering a flexible and reproducible formulation for triggering local cytotoxicity in bladder tumors as a potential replacement for BCG therapy.

Materials and Methods

Materials

Fmoc-protected amino acids, resins, and coupling reagents for solid-phase synthesis were purchased from EMD Millipore. Tris(3-hydroxypropyltriazolylmethyl)amine (THPTA) was purchased from Sigma-Aldrich. 1,2-Dipalmitoyl-*sn*-glycero-3-phosphocholine (DPPC), 1,2-distearoyl-*sn*-glycero-3-phosphoethanolamine (DSPE), 1,2-distearoyl-*sn*-glycero-3-phosphoethanolamine-mPEG1000 (mPEG1000-DSPE), 1,2-distearoyl-*sn*-glycero-3-phosphoethanolamine-PEG2000-azide (N_3-PEG2000-DSPE), and cholesterol (Chol) were purchased from Avanti Polar Lipids. Cyanine 5.5-NHS ester was purchased from Lumiprobe. Cellulose acetate (CA) syringe filters were purchased from Macherey-Nagel Inc. Sephadex® G-50 and LH-20 were purchased from GE Healthcare. LIVE/DEAD® fixable green dead cell stain was purchased from ThermoFisher. AlexaFluor® 680-Wheat Germ Agglutinin conjugate (WGA) and LysoTracker® Blue DND-22 were purchased from Life Technologies. Cell culture reagents such as DMEM, FBS, trypsin, and PBS were purchased from Atlanta Biologicals. Ultrapure water (18 MΩ) was used for preparation of all buffers and in all experiments. All solvents were of analytical grade, purchased from commercial sources and used without further purification, except DMF which was dried over CaH_2 under N_2, filtered, and distilled under reduced pressure.

Peptide Synthesis

The GNRQRWFVVWLGSTNDPV peptide sequence was synthesized following standard solid phase peptide synthesis (SPPS) procedures using the Fmoc-based approach. Gly-Wang resin (300 mg, 0.34 mmol) was swelled inside the reactor with DCM for 20 min before filtration to remove the solvent. The resin-bound amino acid was treated with piperidine (20% in DMF; 20 min) to effect Fmoc deprotection. The resin was filtered and washed two times with DMF, DCM, IPA, and DMF, sequentially. The Fmoc-protected amino acids (6 equiv., 2.04 mmol) were treated with HBTU (6 equiv, 2.04 mmol) and DIEA (12 equiv, 4.08 mmol) and added to the resin for a 1 h reaction period. The resin was then filtered and washed two times with DMF, DCM, IPA, and DMF, sequentially. The coupling and deprotection procedures were repeated until the synthesis of the full peptide sequence was complete. Then, the dried resin was treated with cleavage cocktail (95:2.5:2.5 TFA:H_2O:*i*Pr_3SiH) for 1 h before filtering and washing the resin with fresh cleavage cocktail two times. The filtrates were collected and evaporated using a N_2 stream. Then, an excess amount of water was added and the crude peptide recovered by lyophilization. The peptides were purified using a AKTA Explorer FPLC equipped with a 22/250 C18 preparative column. The dried crude peptide was dissolved in a 6:4 H_2O:ACN mixture and separated by gradient elution with solvent A (ACN + 0.1% TFA) and solvent B (H_2O + 0.1% TFA) at a flow rate (22.9 mL/min) using a 70 min gradient (0–70% solvent A). Fractions containing the desired products were collected (35–45% solvent A), pooled, and lyophilized. The molecular weight of the peptides were confirmed by matrix-assisted laser desorption ionization time-of-flight (MALDI TOF) mass spectrometry using a Voyager DE Pro mass spectrometer.

FAP Peptide-Lipopolymer Synthesis

FAP peptide-lipopolymers (RWFV- and WVRF-containing sequences) were prepared via copper-catalyzed azide-alkyne cycloaddition (CuAAC). A solution containing the alkyne-terminated FAP peptide (0.44 mM in DMF) was added to a 1.5 mL Eppendorf tube, followed by stepwise addition of THPTA (8 mM in water), $CuSO_4$ (5 mM in water), sodium ascorbate (10 mM in water), and N_3-PEG2000-DSPE (1 mM in DMF). The tube was then capped under a stream of N_2 and the mixture subjected to bath sonication for 1 h (37 kHz, 70% power), followed by vigorous agitation with an Eppendorf Thermomixer R (Fisher Scientific, Pennsylvania, USA) (700 rpm, 50 °C) overnight in the dark. The product was collected and purified using a Waters Delta Prep 4000 RP-HPLC equipped with a C8 preparative column (5 × 25 cm). The crude product was separated via gradient elution using solvent A (ACN + 0.1% TFA), solvent B (H_2O + 0.1% TFA), solvent C (MeOH), and solvent D (IPA) at a flow rate of 10 mL/min with a 70 min gradient [0–50 min (5–100% solvent C), 50–55 min (100% solvent C), 55–56 min (100% solvent D), 56–70 min (100% solvent D)]. The molecular weights of the purified FAP peptide-lipopolymers were confirmed by MALDI-TOF.

Cy5.5-DSPE Synthesis

Cy5.5-DSPE was synthesized by direct coupling of Cy5.5-NHS ester with DSPE. DSPE (1 equiv.) was dissolved in dry $CHCl_3$ and Et_3N (4 equiv.) was added to the Cy5.5-NHS ester (2 equiv.) dissolved in DMSO. The two solutions were mixed and heated for 1 h at 50 °C with frequent vortex mixing before incubating in the dark at 22 °C overnight. The crude product was purified by Sephadex® LH-20 column chromatography using 6:4 $CHCl_3$:MeOH as eluent. The fractions of pure Cy5.5-DSPE were collected, pooled, evaporated, and dried under 50 μm vacuum overnight in the dark. The Cy5.5-DSPE molecular weight was confirmed by MALDI-TOF.

Liposome Preparation and Characterization

Liposomes were prepared by the thin-film hydration method. Native FAP peptide-targeted liposomes used GNRQ**RWFV**VWLGSTNDPV-PEG2000-DSPE lipopolymer. Scrambled FAP peptide-targeted liposomes used GNRQ**WVRF**VWLGSTNDPV-PEG2000-DSPE. Non-targeted liposomes used mPEG2000-DSPE. Single PEGylated liposome formulations used DPPC, Chol, Cy5.5-DSPE, and peptidolipopolymer (62.5:35:0.5:2 mol%, respectively; 6 μmol total lipid). Double PEGylated liposome formulations used DPPC, Chol, Cy5.5-DSPE, mPEG1000-DSPE, and peptidolipopolymer (58.5:35:0.5:4:2 mol%, respectively; 6 μmol total lipid). The lipids were mixed in $CHCl_3$ in a glass round bottom flask and slowly evaporated to produce a thin lipid film that was further dried under a 50 μm vacuum overnight. The lipid film was then hydrated with HEPES buffered saline (HBS: 10 mM HEPES, 300 mM sucrose, pH 7.4) at 55 °C and re-suspended by vigorous vortexing. The suspension was transferred to cryogenic vials for ten freeze (−196 °C)/thaw (55 °C)/vortex cycles to enhance the hydration processes. The resulting large multilamellar vesicles were downsized by probe-tip sonication (20 min, output 4), followed by filtration through a 0.2 μm CA syringe filter, to produce small unilamellar vesicles. Separation of the liposomes from unencapsulated material was performed by Sephadex® G-50 size exclusion

chromatography. Particle sizes, size distributions, and ζ-potentials of the different preparations were determined using a Zetasizer Nano S dynamic light scattering device. All measurements were conducted at 25 °C in triplicate and reported as the number mean ± SD. Electron microscopy images of liposomes were collected using a Tecnai T20 transmission electron microscope operating at a 200 kV with a LaB6 filament. Samples were deposited onto Formvar/carbon-coated Cu 400-mesh grids and negatively stained with 2% uranyl acetate prior to visualization.

Liposome Cell Association Analysis

Liposome association with MB49 cells was studied by seeding 10,000 cells per well in 96-well plates and culturing them at 37 °C, 5% CO_2, and 95% relative humidity in complete FBS supplemented DMEM for 24 h to reach 80–90% confluency. Various liposome preparations containing different FAP peptide lipopolymer compositions were incubated with the cells for 1 h at 37 °C under serum-free medium conditions. The unbound liposomes were removed by aspirating the spent medium and washing the cells with PBS (3X). The attached cells were detached by trypsinization and diluted with complete medium at the required concentration for flow cytometric analysis using a Beckman-Coulter FC500. Emission from fluorescein-tagged liposomes were counted using the FL4 channel.

Intracellular Trafficking Study of MB49 Cells After Liposome Exposure

Temporal and spatial tracking of targeted liposomes was studied using multiphoton confocal microscopy. MB49 cells were cultured in complete FBS-supplemented DMEM at a cell density of 35,000 cells/well in 4 chambered slides. After 24 h, the culture media was replaced with serum-free medium containing the FAP peptide-targeted liposomes and incubated for 2 h, followed by removal of the liposome suspension, rinsing of the cells three times with FBS-supplemented DMEM, and incubation for 0 or 10 h at 37 °C. The cells were then stained with AlexaFluor® 680 WGA for 10 min to reveal the plasma membrane, washed with PBS (2X), and then incubated with LysoTracker® Blue DND-22 for 10 min to stain lysosomal compartments, before washing with PBS (2X) and imaging by confocal microscopy with a Nikon A1R MP microscope equipped with a 60X oil immersion objective.

MB49 Cell Viability Assay

Cell viability was measured using LIVE/DEAD® fixable cell stains. MB49 cells were seeded at 10,000 cells per well in 96-well plates in growth medium and allowed to adhere overnight at 37 °C. Cells were washed with PBS and incubated with liposome samples in serum-free media for 1 h. The cells were then washed with PBS, trypsinized, incubated with 0.5 μL stain for 20 min in the dark, and analyzed for their LIVE/DEAD cell fluorescence intensities using the FL1 channel of a Beckman-Coulter FC500 flow cytometer.

Analysis of Liposome Binding to MB49 Bladder Tumors in Mice

All animal experiments followed protocols approved by the Purdue Animal Care and Use Committee (PACUC). Stably transfected luciferase-MB49 cells (MB49-Luc) were instilled via a 31G catheter into the urinary bladders of female mice. All mice were imaged using the

Spectral Ami Optical Imaging System 9–11 days after the tumor implantation procedure to screen for luciferin-induced bioluminescence to determine tumor-associated luminescence intensities and tumor implantation rates. Mice without detectable luminescence were sorted into the control group, whereas tumor-bearing mice were randomly assigned to treatment groups (n = 5 mice/group). At Day 10, 100 μL of each liposome suspension was instilled via catheter into the bladder and allow to in-dwell for 1 h. Liposome suspensions were then removed by aspiration, followed by washing with PBS (5X) *in situ*. A luciferin solution was then injected into the peritoneal cavity 10 min before euthanasia of the animals. Each bladder was excised, inverted to project the tumor-bearing bladder luminal tissue on the outside of the bladder, washed with 45 mL of PBS *ex vivo*, surgically bivalved, and placed on a plastic support with the luminal surface facing up. Luminescence (Field-of-view (FOV): 10 cm, object height: 0.5 cm, exposure time: 120 s, f/stop: 1.2) and fluorescence (FOV: 10 cm, object height: 0.5 cm, excitation: 675 nm, emission: 730 nm, exposure time: 1 s, f/stop: 2) imaging was performed using a Spectral AMI imaging system.

Statistical Analysis

Statistical significance was evaluated by one-way analysis of variance (ANOVA), followed by Dunnett's test for multiple comparison between the FAP peptide-targeted liposome groups and other experimental groups. A p value of < 0.05 was considered to be a statistically significant. *p < 0.05, **p < 0.01, ***p < 0.005, ****p < 0.001.

Supplementary Material

Refer to Web version on PubMed Central for supplementary material.

Acknowledgements

Phase I and Flow Cytometry Shared Resource Facility grant support from the Purdue University Center for Cancer Research (P30 CA023168), NIH Grant R01 GM087016, the Mass Spectrometry Shared Resource, the Bindley Bioscience Imaging Facility, and the Department of Chemistry are greatly acknowledged.

Abbreviations

FBN	fibronectin
FAP	fibronectin attachment protein
BCG	*bovis* bacillus Calmette-Guerin
PEG	poly(ethylene glycol)
DPPC	1,2-Dipalmitoyl-*sn*-glycero-3-phosphocholine
DSPE	1,2-distearoyl-*sn*-glycero-3-phosphoethanolamine
mPEG1000-DSPE	1,2-distearoyl-*sn*-glycero-3-phosphoethanolamine-mPEG1000
N_3-PEG2000-DSPE	1,2-distearoyl-*sn*-glycero-3-phosphoethanolamine-PEG2000-azide

Chol cholesterol

References

(1). Siegel RL, Miller KD, and Jemal A (2015) Cancer statistics, 2015. Ca-Cancer J. Clin 65, 5–29. [PubMed: 25559415]

(2). Jemal A, Tiwari RC, Murray T, Ghafoor A, Samuels A, Ward E, Feuer EJ, Thun MJ, and American Cancer S (2004) Cancer statistics, 2004. Ca-Cancer J. Clin 54, 8–29. [PubMed: 14974761]

(3). Jacobs BL, Lee CT, and Montie JE (2010) Bladder cancer in 2010: How far have we come? Ca-Cancer J. Clin 60, 244–72. [PubMed: 20566675]

(4). Key statistics for bladder cancer. http://www.cancer.org/cancer/bladdercancer/detailedguide/bladder-cancer-key-statistics (accessed March 11).

(5). Clavel J, Cordier S, Boccon-Gibod L, and Hemon D (1989) Tobacco and bladder cancer in males: Increased risk for inhalers and smokers of black tobacco. Int. J. Cancer 44, 605–10. [PubMed: 2793232]

(6). Van der Meijden AP (1998) Bladder cancer. BMJ 317, 1366–9. [PubMed: 9812938]

(7). Anastasiadis A, and de Reijke TM (2012) Best practice in the treatment of nonmuscle invasive bladder cancer. Ther. Adv. Urol 4, 13–32. [PubMed: 22295042]

(8). Brandau S, and Suttmann H (2007) Thirty years of bcg immunotherapy for non-muscle invasive bladder cancer: A success story with room for improvement. Biomed. Pharmacother 61, 299–305. [PubMed: 17604943]

(9). Redelman-Sidi G, Glickman MS, and Bochner BH (2014) The mechanism of action of bcg therapy for bladder cancer--a current perspective. Nat. Rev. Urol 11, 153–62. [PubMed: 24492433]

(10). Zargar H, Aning J, Ischia J, So A, and Black P (2014) Optimizing intravesical mitomycin c therapy in non-muscle-invasive bladder cancer. Nat. Rev. Urol 11, 220–30. [PubMed: 24619373]

(11). Au JLS, Badalament RA, Wientjes MG, Young DC, Warner JA, Venema PL, Pollifrone DL, Harbrecht JD, Chin JL, Lerner SP, et al. (2001) Methods to improve efficacy of intravesical mitomycin c: Results of a randomized phase iii trial. JNCI, J. Natl. Cancer Inst 93, 597–604. [PubMed: 11309436]

(12). Ratliff TL, McCarthy R, Telle WB, and Brown EJ (1993) Purification of a mycobacterial adhesin for fibronectin. Infect. Immun 61, 1889–94. [PubMed: 8478078]

(13). Lilly JD, and Parsons CL (1990) Bladder surface glycosaminoglycans is a human epithelial permeability barrier. Surg., Gynecol. Obstet 171, 493–496. [PubMed: 2244283]

(14). Coon BG, Crist S, Gonzalez-Bonet AM, Kim HK, Sowa J, Thompson DH, Ratliff TL, and Aguilar RC (2012) Fibronectin attachment protein from bacillus calmette-guerin as targeting agent for bladder tumor cells. Int. J. Cancer 131, 591–600. [PubMed: 21901746]

(15). Schorey JS, Holsti MA, Ratliff TL, Allen PM, and Brown EJ (1996) Characterization of the fibronectin-attachment protein of mycobacterium avium reveals a fibronectin-binding motif conserved among mycobacteria. Mol Microbiol 21, 321–329. [PubMed: 8858587]

(16). Zhao W, Schorey JS, Groger R, Allen PM, Brown EJ, and Ratliff TL (1999) Characterization of the fibronectin binding motif for a unique mycobacterial fibronectin attachment protein, fap. J. Biol. Chem 274, 4521–6. [PubMed: 9988684]

(17). Zhao W, Schorey JS, Bong-Mastek M, Ritchey J, Brown EJ, and Ratliff TL (2000) Role of a bacillus calmette-guerin fibronectin attachment protein in bcg-induced antitumor activity. Int. J. Cancer 86, 83–8. [PubMed: 10728599]

(18). Secott TE, Lin TL, and Wu CC (2002) Fibronectin attachment protein is necessary for efficient attachment and invasion of epithelial cells by mycobacterium avium subsp paratuberculosis. Infect. Immun 70, 2670–2675. [PubMed: 11953410]

(19). Hudson MA, Brown EJ, Ritchey JK, and Ratliff TL (1991) Modulation of fibronectin-mediated bacillus calmette-guerin attachment to murine bladder mucosa by drugs influencing the coagulation pathways. Cancer Res. 51, 3726–32. [PubMed: 2065329]

(20). Kavoussi LR, Brown EJ, Ritchey JK, and Ratliff TL (1990) Fibronectin-mediated calmette-guerin bacillus attachment to murine bladder mucosa. Requirement for the expression of an antitumor response. J. Clin. Invest 85, 62–7. [PubMed: 2404029]

(21). Shi F, and Sottile J (2008) Caveolin-1-dependent β1 integrin endocytosis is a critical regulator of fibronectin turnover. J. Cell Sci 121, 2360. [PubMed: 18577581]

(22). Zhu L, and Torchilin VP (2013) Stimulus-responsive nanopreparations for tumor targeting. Integr. Biol 5, 101039/c2ib20135f.

(23). Perche F, and Torchilin VP (2013) Recent trends in multifunctional liposomal nanocarriers for enhanced tumor targeting. J. Drug Delivery 2013, 705265.

(24). Çağdaş M, Sezer AD, and Bucak S (2014) Liposomes as potential drug carrier systems for drug delivery, InTech.

(25). Torchilin V (2009) Multifunctional and stimuli-sensitive pharmaceutical nanocarriers. Eur. J. Pharm. Biopharm 71, 431–444. [PubMed: 18977297]

(26). Barenholz Y (2012) Doxil® — the first fda-approved nano-drug: Lessons learned. J. Controlled Release 160, 117–134.

(27). Felber AE, Dufresne M-H, and Leroux J-C (2012) Ph-sensitive vesicles, polymeric micelles, and nanospheres prepared with polycarboxylates Adv. Drug Delivery Rev 64, 979–992.

(28). Bovis MJ, Woodhams JH, Loizidou M, Scheglmann D, Bown SG, and MacRobert AJ (2012) Improved in vivo delivery of m-thpc via pegylated liposomes for use in photodynamic therapy. J. Controlled Release 157, 196–205.

(29). Thamphiwatana S, Fu V, Zhu J, Lu D, Gao W, and Zhang L (2013) Nanoparticle-stabilized liposomes for ph-responsive gastric drug delivery. Langmuir 29, 12228–12233. [PubMed: 23987129]

(30). Nakamura T, Noma Y, Sakurai Y, and Harashima H (2017) Modifying cationic liposomes with cholesteryl-peg prevents their aggregation in human urine and enhances cellular uptake by bladder cancer cells. Biol. Pharm. Bull 40, 234–237. [PubMed: 28154264]

(31). Vila-Caballer M, Codolo G, Munari F, Malfanti A, Fassan M, Rugge M, Balasso A, de Bernard M, and Salmaso S (2016) A ph-sensitive stearoyl-peg-poly(methacryloyl sulfadimethoxine)-decorated liposome system for protein delivery: An application for bladder cancer treatment. J. Controlled Release 238, 31–42.

(32). Lin T. y., Li Y-P, Zhang H, Luo J, Goodwin N, Gao T, de Vere White R, Lam KS, and Pan C-X (2013) Tumor-targeting multifunctional micelles for imaging and chemotherapy of advanced bladder cancer. Nanomedicine (London, U. K.) 8, 1239–1251.

(33). Derycke AS, Kamuhabwa A, Gijsens A, Roskams T, De Vos D, Kasran A, Huwyler J, Missiaen L, and de Witte PA (2004) Transferrin-conjugated liposome targeting of photosensitizer alpcs4 to rat bladder carcinoma cells. J. Natl. Cancer Inst 96, 1620–30. [PubMed: 15523091]

(34). Ay Şenyiğit Z, Karavana SY, İlem-Özdemir D, Çalışkan Ç, Waldner C, Şen S, Bernkop-Schnürch A, and Baloğlu E (2015) Design and evaluation of an intravesical delivery system for superficial bladder cancer: Preparation of gemcitabine hcl-loaded chitosan–thioglycolic acid nanoparticles and comparison of chitosan/poloxamer gels as carriers. Int. J. Nanomed 10, 6493–6507.

(35). Wilson-Ashworth HA, Bahm Q, Erickson J, Shinkle A, Vu MP, Woodbury D, and Bell JD (2006) Differential detection of phospholipid fluidity, order, and spacing by fluorescence spectroscopy of bis-pyrene, prodan, nystatin, and merocyanine 540. Biophys. J 91, 4091–101. [PubMed: 16980369]

(36). Verma A, and Stellacci F (2010) Effect of surface properties on nanoparticle-cell interactions. Small 6, 12–21. [PubMed: 19844908]

(37). Horn JN, Romo TD, and Grossfield A (2013) Simulating the mechanism of antimicrobial lipopeptides with all-atom molecular dynamics. Biochemistry 52, 5604–10. [PubMed: 23875688]

(38). Forssen E, and Willis M (1998) Ligand-targeted liposomes. Adv Drug Deliver Rev 29, 249–271.

(39). Elias DR, Poloukhtine A, Popik V, and Tsourkas A (2013) Effect of ligand density, receptor density, and nanoparticle size on cell targeting. Nanomedicine 9, 194–201. [PubMed: 22687896]

(40). Longo GS, Thompson DH, and Szleifer I (2008) Ligand-receptor interactions between surfaces: The role of binary polymer spacers. Langmuir 24, 10324–33. [PubMed: 18698869]

(41). Garnacho C (2016) Intracellular drug delivery: Mechanisms for cell entry. Curr. Pharm. Des 22, 1210–26. [PubMed: 26675221]

(42). Ohki K, Kumagai K, Mitsuda S, Takano T, Kimura T, and Ikuta K (1993) Characterization of a unique scrambled peptide derived from the cd4 cdr3-related region which shows substantial activity for blocking hiv-1 infection. Vaccine 11, 682–686. [PubMed: 8322494]

(43). Perfetto SP, Chattopadhyay PK, Lamoreaux L, Nguyen R, Ambrozak D, Koup RA, and Roederer M (2010) Amine-reactive dyes for dead cell discrimination in fixed samples. Curr. Protoc. Cytom CHAPTER, Unit-9.34.

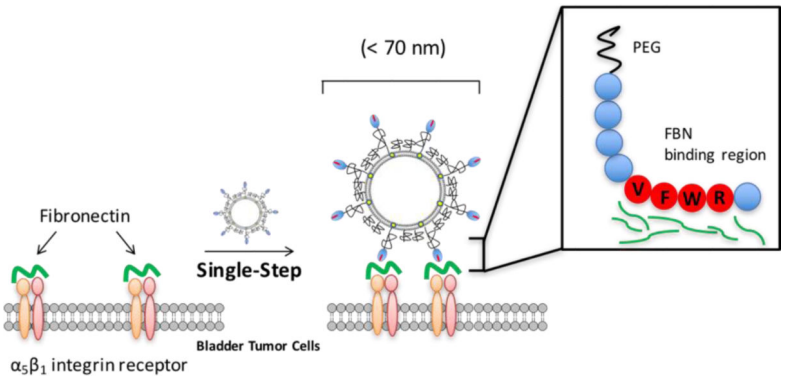

Figure 1.

Conceptual diagram of FAP peptide-targeted liposome binding to exposed fibronectin-integrin complexes on the surface of bladder tumor cells.

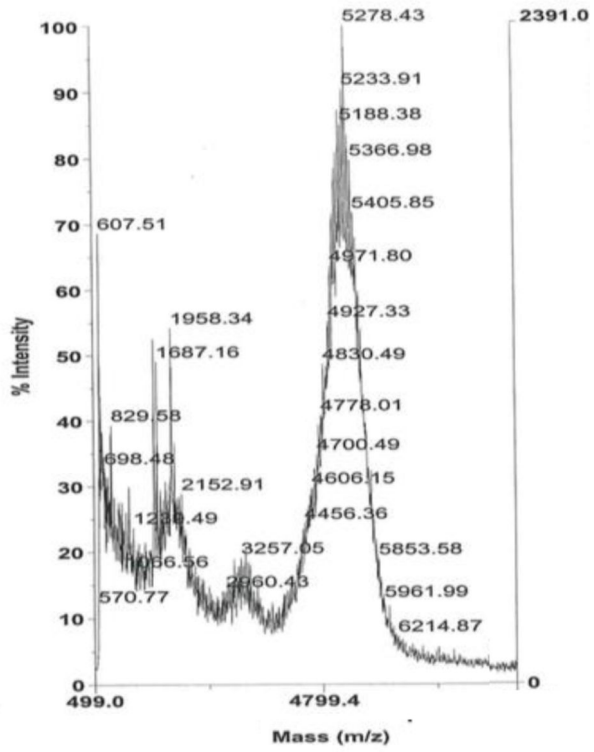

Figure 2.
MALDI-TOF mass spectrum of the RWFV-PEG2000-DSPE conjugate.

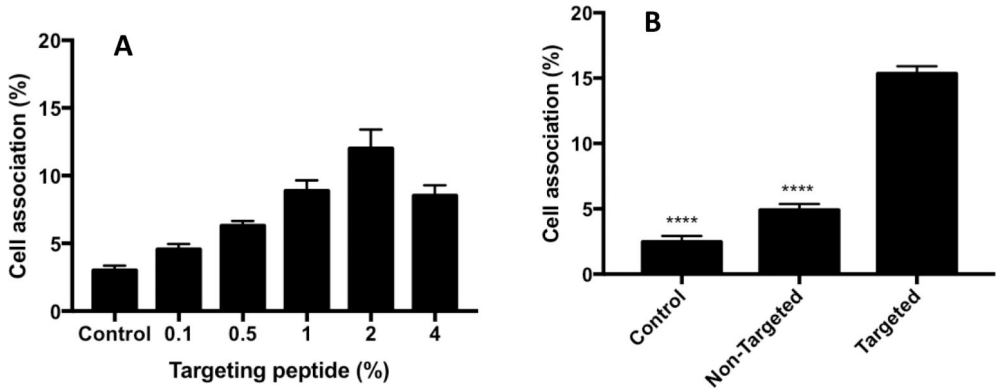

Figure 3.

A: Evaluation of cell association mediated by liposomes bearing FAP peptide-lipopolymer at various membrane loading densities (0.1, 0.5, 1, 2, 4 mol%). MB49 cells were treated with Cy5.5-labeled liposomes bearing different concentrations of RWFV-PEG2000-DSPE and incubated for 1 h at 37 °C. The media was then aspirated and the cells washed with PBS, trypsinized, and analyzed by flow cytometry for the number of cells displaying Cy5.5 fluorescence. Liposome diameters: 55–65 nm. Liposome composition: 64.5-x:35:x:0.5 DPPC:Chol:RWFV-PEG2000-DSPE:Cy5.5-DSPE. Control: no liposome treatment. Error bars indicate the standard deviation of the mean with n=3. **B:** Comparison of cell association events between 2 mol% targeted (RWFV-PEG2000-DSPE) and non-targeted (mPEG2000-DSPE) liposomes in MB49 cells. The liposomes were incubated with cells for 1 h at 37 °C, followed by media aspiration, washing with PBS, trypsinization, and flow cytometry analysis for Cy5.5 fluorescence. Liposome diameters: 58 nm. Liposome composition (targeted): 62.5:35:2:0.5 DPPC:Chol:RWFV-PEG2000-DSPE:Cy5.5-DSPE. Liposome composition (non-targeted): 62.5:35:2:0.5 DPPC:Chol:mPEG2000-DSPE:Cy5.5-DSPE. Control: no liposome treatment. Error bars indicate the standard deviation of the mean with n=3 (ANOVA: *p < 0.05, **p < 0.01, ***p < 0.005, ****p < 0.001).

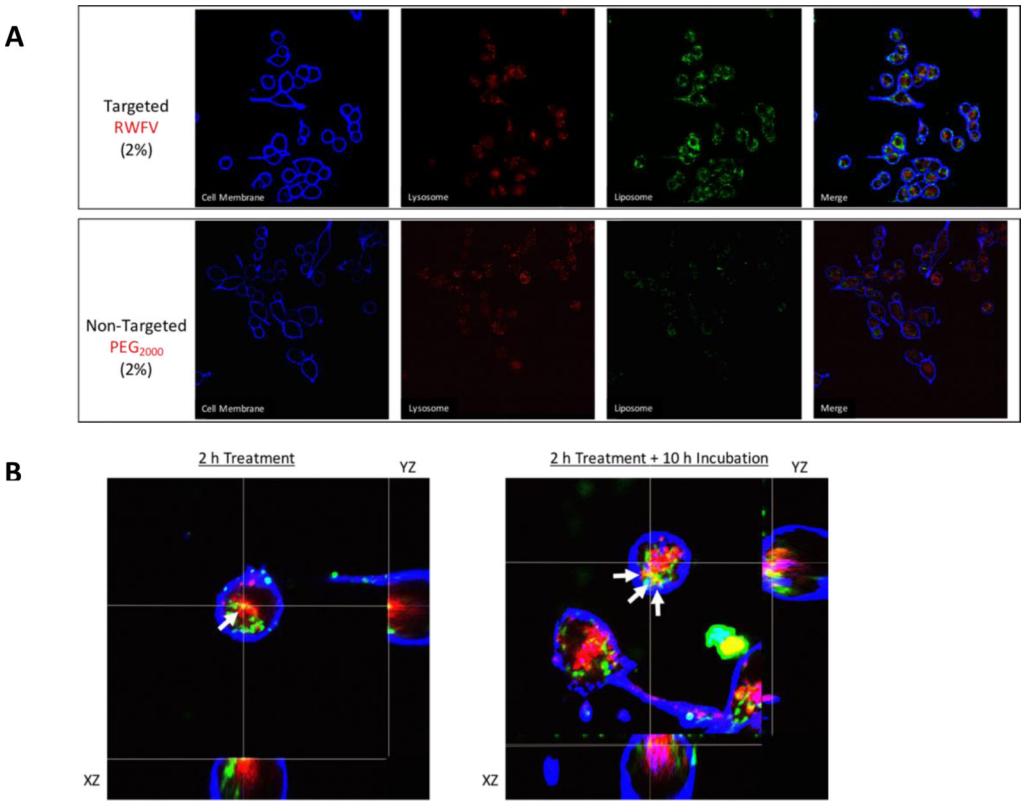

Figure 4.

A: Binding and intracellular trafficking of targeted (top) and non-targeted (bottom) liposomes in MB49 murine bladder tumor cells. MB49 cells were treated with liposome formulations in serum-free medium for 2 h at 37 °C prior to imaging by confocal microscopy. Targeted liposome composition: 62.5:35:2:0.5 DPPC:Chol:RWFV-PEG2000-DSPE:Cy5.5-DSPE. Non-targeted liposome composition: 62.5:35:2:0.5 DPPC:Chol:mPEG2000-DSPE:Cy5.5-DSPE. **B:** MB49 cells were treated with targeted liposomes (2 mol% RWFV-PEG2000-DSPE) for 2 h, followed by incubation for additional 0 h (left) or 10 h (right). Acidic lysosomes were stained with LysoTracker® Blue DND-22 and plasma membranes were stained with AlexaFluor® 680 WGA. Arrows indicate regions of coincident LysoTracker and FITC fluorescence, indicating the co-localization of FITC-labeled liposomes within acidic late endosome/lysosome compartments. Liposome diameters: 58 nm. Liposome composition: 62.5:35:2:0.5 DPPC:Chol:RWFV-PEG2000-DSPE:Cy5.5-DSPE.

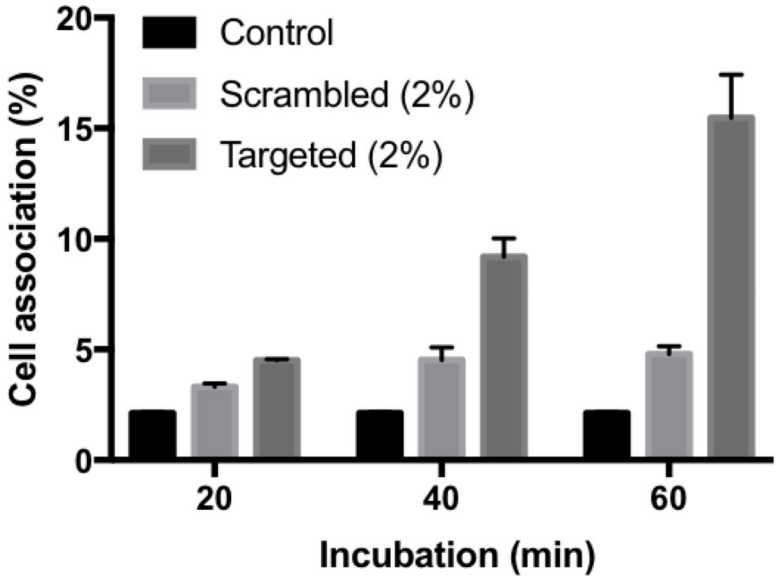

Figure 5.

Evaluation of targeting specificity using targeted and scrambled FAP peptide-lipopolymer liposomes in MB49 cells. The liposomes were incubated with cells for 20, 40, and 60 min at 37 °C. Then media was aspirated and cells were washed with PBS, trypsinized, and analyzed by flow cytometry for Cy5.5 fluorescence as a measure of cell binding. Liposome diameter: 52 nm. Targeted liposome formulation: 62.5:35:2:0.5 DPPC:Chol:RWFV-PEG2000-DSPE:Cy5.5-DSPE. Scrambled liposome formulation: 62.5:35:2:0.5 DPPC:Chol:WVRF-PEG2000-DSPE:Cy5.5-DSPE. Control: no liposome treatment. Error bars indicate the standard deviation of the mean with n=3.

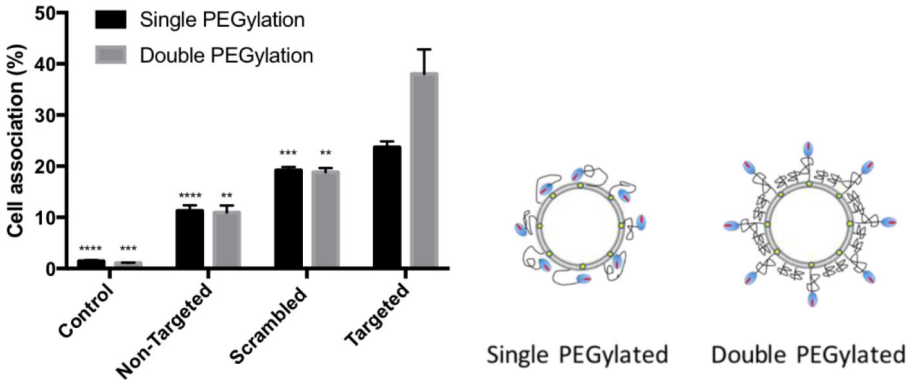

Figure 6.

Cell association of single and double PEGylated liposomes incorporating different functionalized FAP peptide-lipopolymers (non-targeted, 2 mol% mPEG2000-DSPE; scrambled, 2 mol% WVRF-PEG2000-DSPE; and targeted, 2 mol% RWFV-PEG2000-DSPE) in MB49 cells. mPEG1000-DSPE (4 mol%) was included in the liposome formulation to reduce non-specific binding and enhance targeting efficiency. The liposomes were incubated with cells for 1 h at 37 °C. Then, the media was aspirated, the cells washed with PBS, and trypsinized before flow cytometry analysis of Cy5.5 fluorescence as a measure of cell binding. Liposome diameter: 58 nm. Liposome formulation: 58.5:35:4:2:0.5 DPPC:Chol:mPEG1000-DSPE:X:Cy5.5-DSPE, where X = RWFV-PEG2000-DSPE (targeted), WVRF-PEG2000-DSPE (scrambled), or mPEG2000-DSPE (non-targeted). Control: no liposome treatment. Error bars indicate the standard deviation of the mean with n=3. **Right:** Conceptual diagram of FAP peptide ligand presentation on single vs. double PEGylated liposome surfaces.

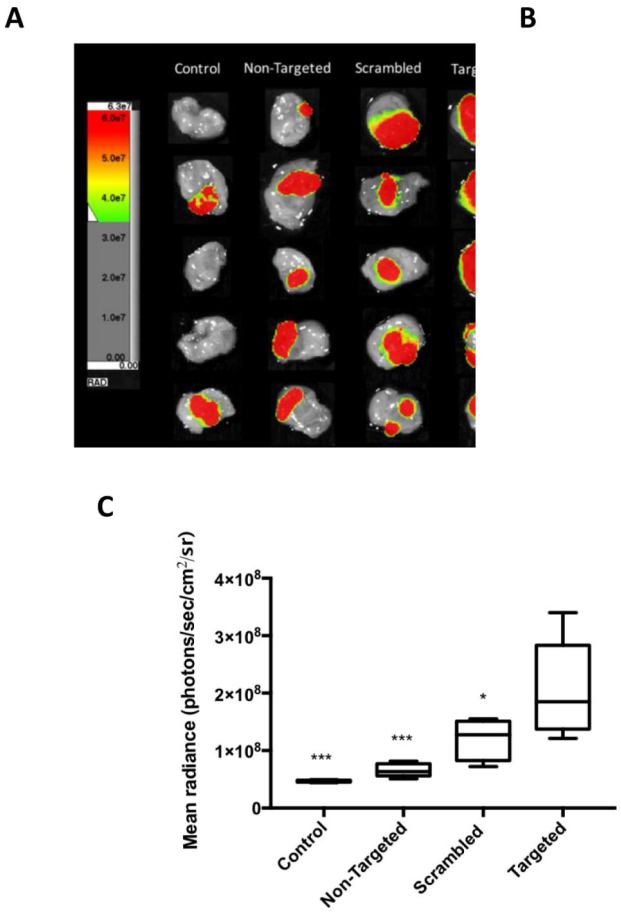

Figure 7.

In vivo bladder tumor tissue targeting evaluation using double PEGylated liposomes incorporating different functionalized lipopolymers (non-targeted, 2 mol% mPEG2000-DSPE; scrambled, 2 mol% WVRF-PEG2000-DSPE; or targeted, 2 mol% RWFV-PEG2000-DSPE) versus untreated controls. **A:** Luciferin-induced luminescence signal from MB49-Luc bladder tumor cells; **B:** Cy5.5 fluorescence arising from liposomes bound to bladder tissue; and **C:** Mean radiance (whole bladder ROI's) of control and treated tissues using different liposome preparations. The liposomes were instilled into the bladder intravesically and allowed to in-dwell for 1 h before aspirating the liposome suspension and washing the bladder with PBS. Luciferin was then injected i.p. before euthanasia. The bladder was then harvested, inverted, washed, and placed for imaging. Liposome diameter: 61 nm. Liposome formulation: 58.5:35:4:2:0.5 DPPC:Chol:mPEG1000-DSPE:X:Cy5.5-DSPE, where X = mPEG2000-DSPE (non-targeted); WVRF-PEG2000-DSPE (scrambled); or RWFV-PEG2000-DSPE (targeted). Control: no liposome treatment. Error bars indicate the standard deviation of the mean with n=5 (ANOVA: *p < 0.05, **p < 0.01, ***p < 0.005, ****p < 0.001).